Ab Initio Molecular Orbital Study of the Reactivity of Active Alkyl Groups. V. Nitrosation Mechanism of Acetone with *syn*-Form of Methyl Nitrite

Tokihiro NIIYA,* Hirohito IKEDA, Miho YUKAWA, and Yoshinobu GOTO

Faculty of Pharmaceutical Sciences, Fukuoka University; Nanakuma, Jonan-ku, Fukuoka 814–0180, Japan.
Received June 17, 2002; accepted September 2, 2002

The mechanisms of nitrosation of acetone through sodium enolate $[CH_3CO^1CH_2]^-Na^+$ (1) or naked enolate $[CH_3CO^1CH_2]^-$ (2) with methyl nitrite $CH_3O^3NO^2$ (3), and the reactivity of the *syn*-form of 3 (*syn*-3) during the C–N bond formation process were investigated using *ab initio* molecular orbital (MO) methods. Our results have demonstrated the predominant formation of *E*-1-hydroxyimino-2-oxo-propane $CH_3COCH{=}NOH$ (4*E*) when the complex $[CH_3CO^1CH_2NO^2(O^3CH_3)]^-Na^+$ was produced kinetically *via* a metal-chelated pericyclic transition state ($TS_{CHELATED}$), in which the O^3 atom of *syn*-3 was coordinated to the Na^+ atom of 1.

Key words nitrosation mechanism; *ab initio* MO method; methyl nitrite; *syn*-form; pericyclic transition state; open-chain transition state

For the nitrosation of active alkyl compounds $RCOCH_2R'$ using alkyl nitrite R″ONO in the presence of base catalyst B^-M^+ to give *E*- and *Z*-hydroxyimino compound $RCOCR'{=}NOH$ (Eq. 1), the rate-determining step of the nitrosation is the C–N bond formation.

$$RCOCH_2R' + R''ONO \xrightarrow{B^-M^+} RCOCR'{=}NOH + R''OH \quad (1)$$

In the case of the nitrosation of the methyl or ethyl group of carbonyl compounds, such as acetone and 2-butanone, the *E*-form of the hydroxyimino compound was predominantly obtained.[1—3] On the other hand, a *E*-form/*Z*-form (*E*/*Z*) ratio of 2.3 was observed for the nitrosation of 3-methyl-1-phenylbutan-1-one ($PhCOCH_2CH(CH_3)_2$) (**5**) with *tert*-butyl nitrite in THF.[4] Thus the *E*/*Z* ratio decreased with increasing bulkiness of the R and R′ groups of $RCOCH_2R'$.

As shown in Fig. 1, alkyl nitrite R″ONO exists as either the *syn*- or *anti*-conformer. The proportion of the *anti*-form of R″ONO was found to increase in the order $R''{=}CH_3$<primary<secondary<tertiary.[5] The *E*/*Z* ratio of the hydroxyimino compound increased when methyl nitrite (**3**) was used in place of *tert*-butyl nitrite in the nitrosation of **5**,[6] which indicated that the *E*/*Z* ratio is affected by the conformation of R″ONO. Our experimental and theoretical investigations on the mechanisms of nitrosation have shown that the *E*/*Z* ratio varied significantly with the participation of the counter cation M^+ of the base catalyst.[4,7,8] Consequently, two types of transition state models (TS) during the C–N bond formation process were proposed to elucidate the variation of the *E*/*Z* ratio in various solvents; specifically, the TS models were 1) metal-chelated pericyclic transition state ($TS_{CHELATED}$) and 2) open-chain transition state without metal (TS_{OPEN}).[4,7] Previous calculations of the nitrosation of sodium enolate $[CH_3COCH_2]^-Na^+$ (**1**) with the *anti*-form of **3** (*anti*-**3**) have shown that *Z*-1-hydroxyimino-2-oxo-propane (**4***Z*) was obtained predominantly, with the nitrosation proceeding *via* $TS_{CHELATED}$.[4] In the case of naked enolate $[CH_3COCH_2]^-$ (**2**), the reaction with *anti*-**3** afforded not only **4***Z* but also **4***E* *via* TS_{OPEN}.[7]

In the present study, the mechanisms of the stereochemical nitrosation of **1** or **2** with *syn*-form of **3** (*syn*-**3**), as opposed to *anti*-**3**, were investigated by *ab initio* MO methods using the same two transition state models as described above.[4,7] Our studies have shown the predominant formation of **4***E* when the complex $[CH_3COCH_2NO(OCH_3)]^-Na^+$ was produced *via* $TS_{CHELATED}$, with the O^3 atom of *syn*-**3** coordinated to the Na^+ atom of **1**. On the other hand, similar coordination between the O^3 atom of *anti*-**3** to the Na^+ atom of **1** was not observed in TS, as described in the previous paper.[4]

Experimental

Computational Procedures MO calculations were carried out using the Gaussian 98 program.[9] The optimized geometries in the TS were initially determined using HF/6-31G, followed by intrinsic reaction coordinate (IRC) calculations. For the energies of the complexes, calculations were performed using similar methods, MP3/6-31+G//HF/6-31G, as previously described.[4] The structure of *syn*-**3** was used to provide the initial geometries for the C–N bond formation process.

Results and Discussion

For the studies on the nitrosation mechanisms between **3** and **1** or **2**, $TS_{CHELATED}$ or TS_{OPEN} models, respectively, were adopted for the C–N bond formation process. In this report, the influence of the conformation of alkyl nitrite on the nitrosation mechanism was investigated using *syn*-**3**, as opposed to *anti*-**3**, which was described in previous papers.[4] As shown in Chart 1, MO calculations for the formation of **4** were carried out stepwise as follow: The nitrosation of **1** or **2** with *syn*-**3** (Eq. 2) to yield **4** was divided into two processes, the C–N bond forming process *via* $TS_{CHELATED}$ (Eq. 3-1) or *via* TS_{OPEN} (Eq. 3-2), the final elimination process shown as Eq. 4. MO calculations were carried out for Eq. 3-1 and 3-2, followed by the elimination processes (Eq. 4). Two pathways (paths A, B) were considered with $TS1_{Na}$-A and -B in Fig. 2 arising from the difference of the geometrical orientation of **3** toward **1**.[4] Initially, the geometries of the transition states ($TS1_{Na}$ or TS1) were determined, and subsequently those of

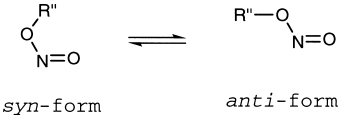

Fig. 1. Conformers of Alkyl Nitrite, R″ONO

* To whom correspondence should be addressed. e-mail: niiya@fukuoka-u.ac.jp

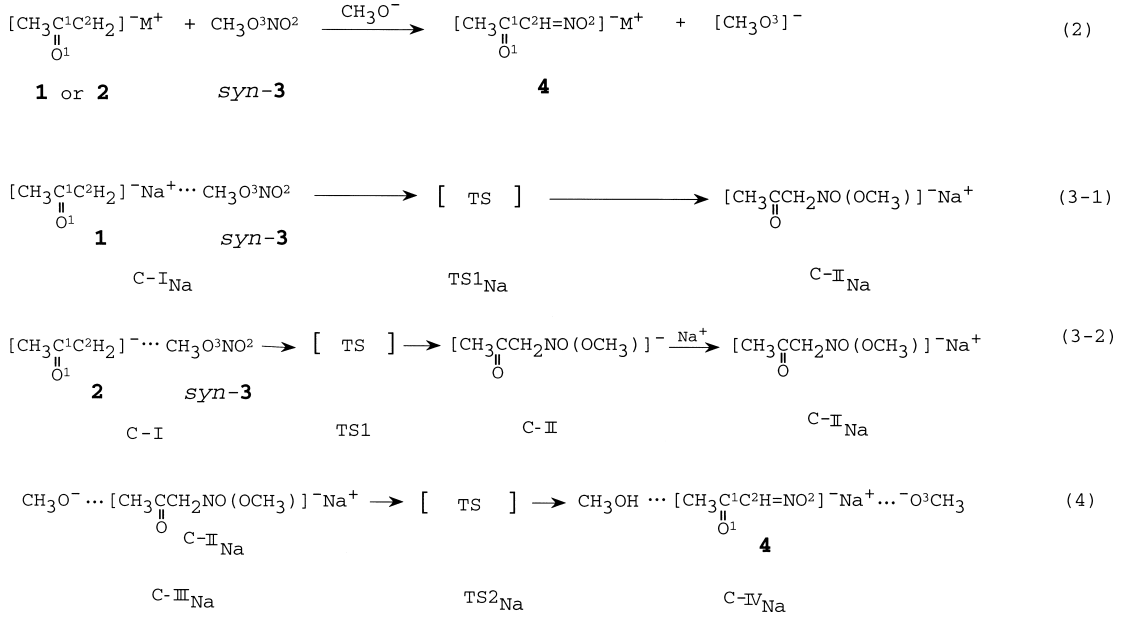

Chart 1

$C\text{-}I_{Na}$ and $C\text{-}II_{Na}$ (or C-I and C-II) were obtained from $TS1_{Na}$ (or TS1) using the IRC method, respectively. The active hydrogen atom in the H–C^2 bond of $C\text{-}II_{Na}$ was attacked by the base CH_3O^-, followed by demethoxylation occurred, and lastly by deprotonation to give $C\text{-}IV_{Na}$. The details of the complexes ($C\text{-}I_{(Na)}$—$C\text{-}IV_{Na}$) in Chart 1 were described below.

For the calculation of the geometry of $TS_{CHELATED}$, two types of the $TS1_{Na}$ complex ($TS1_{Na}$–O^2 and $TS1_{Na}$–O^3) were obtained. The terms $TS1_{Na}$–O^2 and $TS1_{Na}$–O^3 refer to the complexes in which the O^2 atom and O^3 atom of *syn*-**3**, respectfully, are coordinated to the Na^+ atom of **1**. In the case of the nitrosation of **1** with *anti*-**3**, the O^3 atom in *anti*-**3** did not coordinate to the Na^+ atom in the TS, as described previously.[4] The differences of the behavior between *syn*-**3** and *anti*-**3** in the TS can be explained as steric influence of the methyl group of **3**. In the case of nitrosation of **1** using *anti*-**3**, the negative charge of the O^2 atom in *anti*-**3** increased with the decreasing distance of C^2–N bond between **1** and **3**, and hence the binding site of Na^+ migrated more easily from O^3 atom to the O^2 atom as the reaction proceeded.

C–N Bond Formation of the Sodium Enolate of Acetone with *syn*-Form of Methyl Nitrite *via* $TS_{CHELATED}$ The geometries, bond parameters (Å), and calculated energies of the optimized complexes, $C\text{-}I_{Na}$, $TS1_{Na}$ and $C\text{-}II_{Na}$, are shown in Figs. 2 and 3. The complexes $C\text{-}II_{Na}$–O^2-A and -B were derived from $C\text{-}I_{Na}$–O^2 consisted of **1** and *syn*-**3** *via* $TS1_{Na}$–O^2-A (path A) and -B (path B), respectively, as shown in Fig. 2. The complexes $C\text{-}II_{Na}$–O^3-A and -B were derived from $C\text{-}I_{Na}$–O^3 *via* $TS1_{Na}$–O^3-A (path A) and -B (path B), respectively, as shown in Fig. 3. (Eq. 3-1). The designations, $C\text{-}I_{Na}$–O^2 and $C\text{-}I_{Na}$–O^3, refer to complex $C\text{-}I_{Na}$ with coordination between the Na^+ atom of **1** to the O^2 or O^3 atoms, respectively, of *syn*-**3**. The energies (kcal), which are shown in parenthesis, are the differences between the energies of $TS1_{Na}$ and $C\text{-}I_{Na}$, specifically, the activation energies during the C–N bond formation process. Among the available paths, path A in Fig. 3 (4.74 kcal) was kinetically the most favorable path in the formation of $C\text{-}II_{Na}$. The final geometries of CH_3COCH_2NO moieties for each $C\text{-}II_{Na}$ structures (Figs. 2, 3) show completion of the C–N bond formation. The transformation from $TS1_{Na}$ to $C\text{-}II_{Na}$ also involved structural changes in the $[CH_3COCH_2]^-Na^+$ moiety, from the enol- to the keto-form. In the structures of $C\text{-}II_{Na}$–O^2-A and $C\text{-}II_{Na}$–O^3-A, two leaving groups, CH_3O^3 and H^2, were arranged nearly antiperiplanar to one another ($\angle H^2C^2NO^3 = 174.8°$, 137.9°), respectively. This conformation indicated that the elimination reaction of these groups was facile with non-energy barrier. The structure of $C\text{-}II_{Na}$–O^2-A was similar to that of the complex produced in the nitrosation of **1** with *anti*-**3**.[4] The eliminations of CH_3O^3 group and H^2 atom in $C\text{-}II_{Na}$–O^2-A with a base afforded **4***Z*, as described in the previous paper.[4] The N–O^3 bond length in both $C\text{-}II_{Na}$–O^3-A and $C\text{-}II_{Na}$–O^3-B was shown to be considerably extended during the C–N bond formation process.

C–N Bond Formation of the Naked Enolate of Acetone with *syn*-Form of Methyl Nitrite *via* TS_{OPEN} The geometries, bond parameters (Å), and calculated energies of the optimized complexes (C-I, TS1, C-II, and $C\text{-}II_{Na}$) derived *via* TS_{OPEN} and both paths (A and B; Eq. 3-2) are shown in Fig. 4. The geometry of $C\text{-}II_{Na}$-B is the mirror image of that of $C\text{-}II_{Na}$–O^2-A, and therefore the complex $C\text{-}II_{Na}$-B, as well as $C\text{-}II_{Na}$–O^2-A, afforded **4***Z* *via* the subsequent elimination reaction, as described previously.[4] The two leaving groups, CH_3O^3 and H^1, in $C\text{-}II_{Na}$-A were nearly antiperiplanar to one another. The conformation of $C\text{-}II_{Na}$-A indicated that the subsequent elimination reaction can easily occur with non-energy barrier to afford **4***E*.

Elimination of Methoxide and Proton from C–II_{Na} with a Base Figure 5 shows the geometries and calculated energies of $C\text{-}IV_{Na}$ complexes, which were derived from the corresponding $C\text{-}II_{Na}$ with non-energy barrier in the elimination processes. Initially, the CH_3O^3 group of $C\text{-}II_{Na}$–O^2-A, as well as that in $C\text{-}II_{Na}$-B, was eliminated using base CH_3O^-, followed by deprotonation of the active hydrogen atom of the H–C^2 bond to yield **4***Z* as shown in $C\text{-}IV_{Na}$–O^2-A. Similarly,

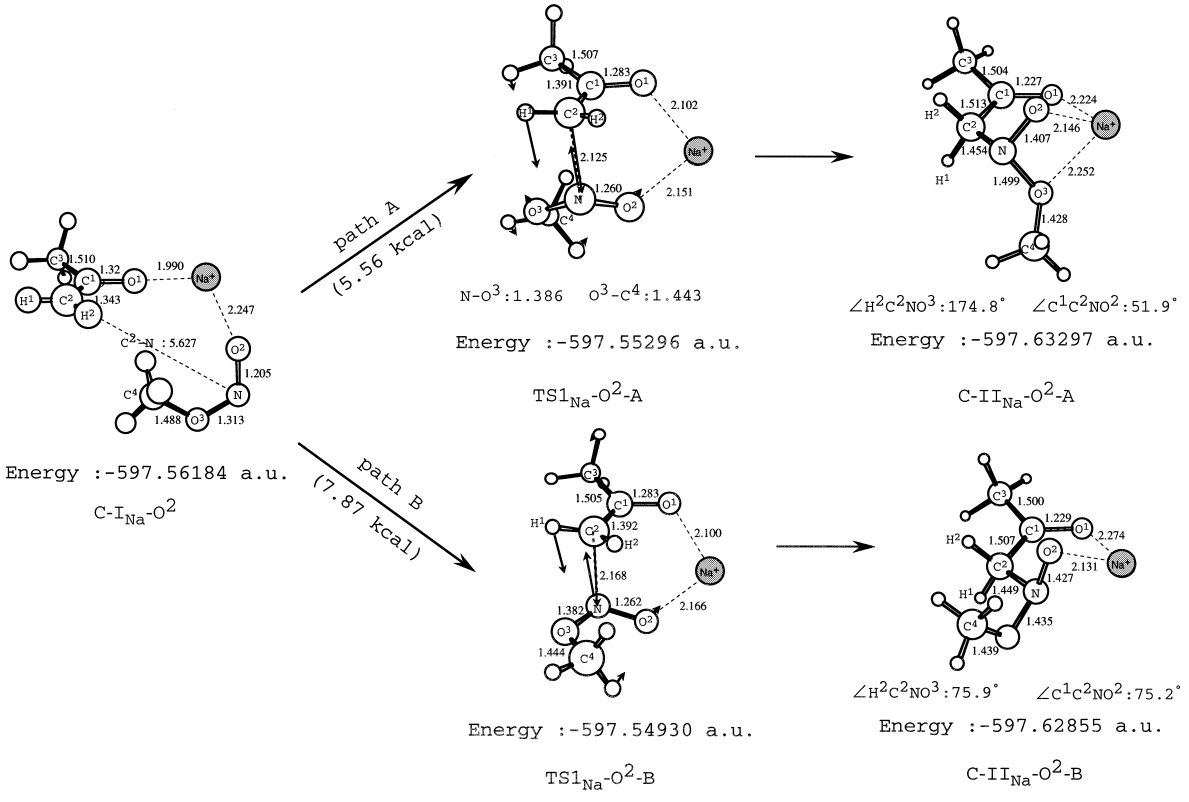

Fig. 2. C–N Bond Formation Process of Nitrosation of Sodium Enolate of Acetone with *syn*-**3** *via* TS1$_{Na}$–O^2

Imaginary frequency modes are shown with bold arrows in the structures of the transition states.

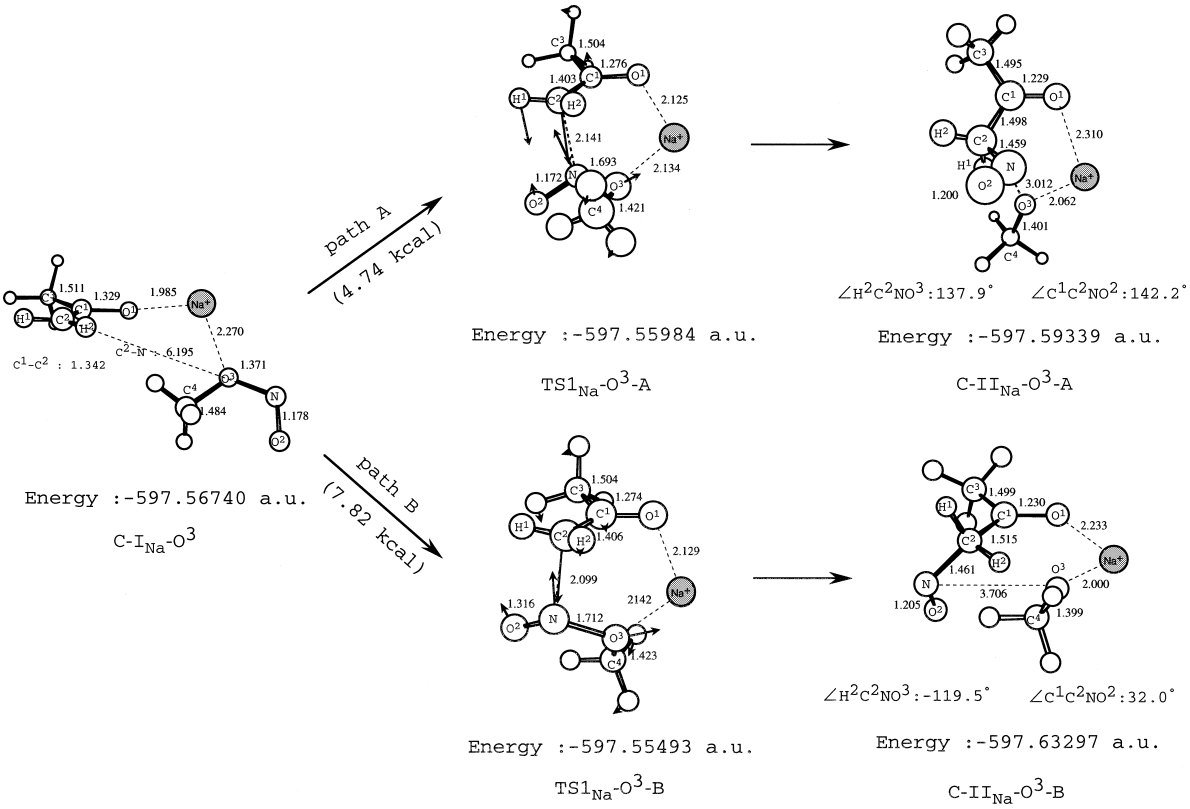

Fig. 3. C–N Bond Formation Process of Nitrosation of Sodium Enolate of Acetone with *syn*-**3** *via* TS1$_{Na}$–O^3

Imaginary frequency modes are shown with bold arrows in the structures of the transition states.

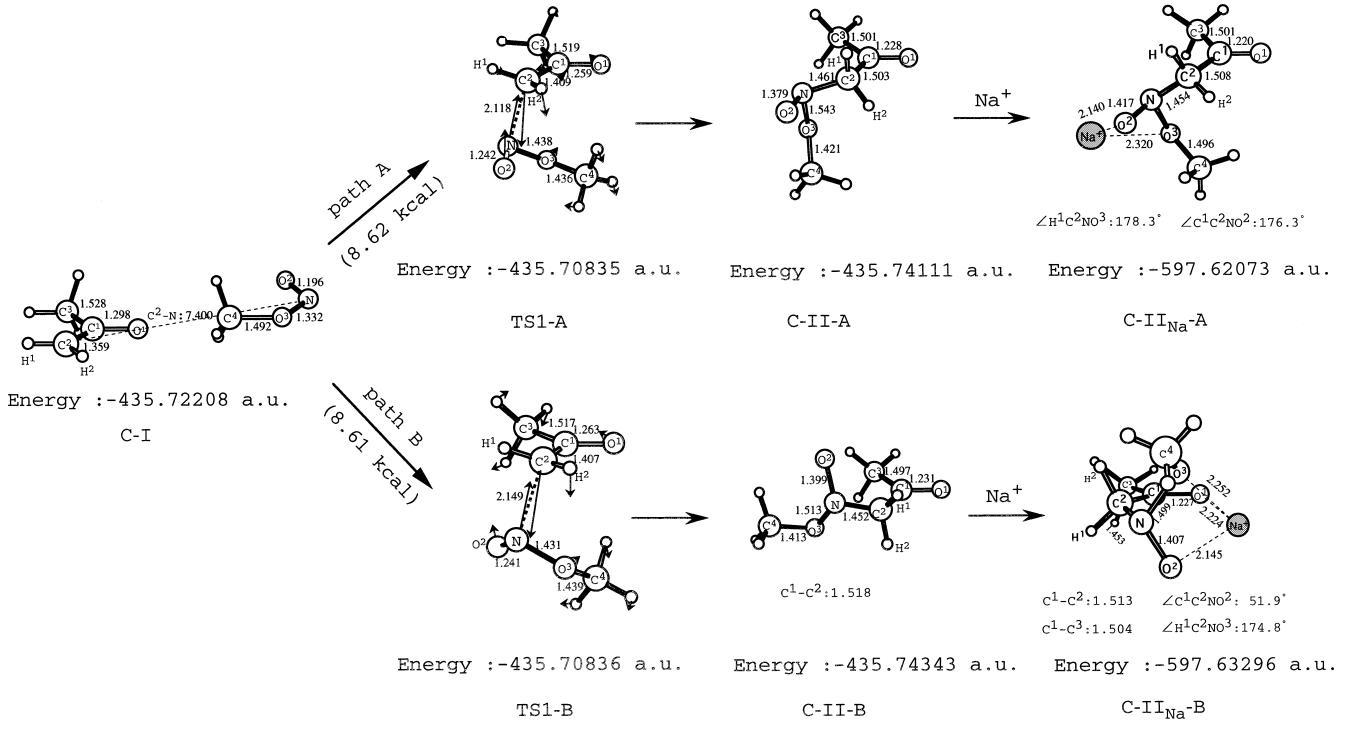

Fig. 4. C–N Bond Formation Process of Nitrosation of Naked Enolate of Acetone with *syn*-**3** *via* TS_{OPEN}
Imaginary frequency modes are shown with bold arrows in the structures of the transition states.

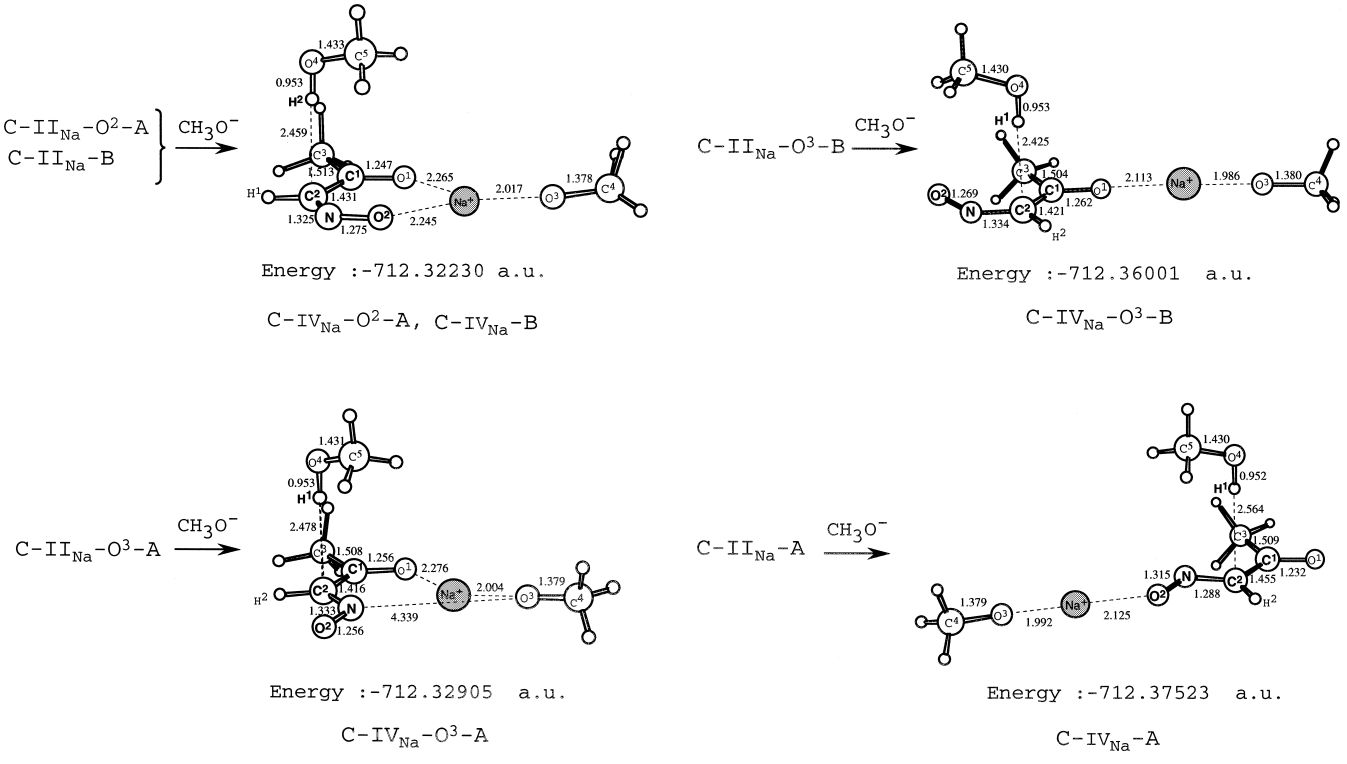

Fig. 5. Elimination Process of Nitrosation

C-IV$_{Na}$–O^3-B was obtained as **4***Z* from C-II$_{Na}$–O^3-B. In contrast, although the elimination reaction proceeded through mechanisms similar as that for C-II$_{Na}$–O^2-A, C-IV$_{Na}$–O^3-A was obtained as **4***E* from C-II$_{Na}$–O^3-A. C-IV$_{Na}$-A was obtained as **4***E* from C-II$_{Na}$-A. As a note, hydroxyimino compound **4** was not formed in the elimination process of C-II$_{Na}$–O^2-B with a base.

Concluding Remarks

Our studies have shown that the complex C-II$_{Na}$–O$_3$-A was

formed kinetically most readily as the intermediate of the reaction between **1** and *syn*-**3** *via* $TS_{CHELATED}$, with the O^3 atom coordinated to the Na^+ atom. The active hydrogen atom of the H–C^2 bond in C-II_{Na}–O^3-A reacted with base CH^3O^-, and the reaction induced the demethoxylation of **3** moiety in C-II_{Na}–O^3-A with non-energy barrier, followed by deprotonation to give **4***E*. **4***E* was obtained from the other complex, C-II_{Na}-A, which consisted of the naked enolate **2** and *syn*-**3**. For the formation of **4***E* in the nitrosation of CH_3COCH_3 with **3**, the geometry of **3** in the complex must be in the *syn*-form during the process of the formation of C-II_{Na}. Furthermore, it is required that the O^3 atom of *syn*-**3** moiety is coordinated to the Na^+ atom in these complexes.

The *E*/*Z* ratio of the hydroxyimino compound decreases when *tert*-butyl nitrite having a predominant *anti*-form is used in place of *syn*-**3** in the nitrosation, since the O^3 atom in *tert*-butyl nitrite does not coordinate to the Na^+ atom in the TS unless the conformation is transformed by the steric hindrance.

Acknowledgements Thanks are due to the Information Technology Center of Fukuoka University for use of the Fujitsu GP7000SModel1000 computer, and to the Research Center for Computational Science, Okazaki National Research Institutes for use of the NEC SX5 and Fujitsu VPP5000 computers, and to the Computing and Communications Center of Kyushu University for use of the Fujitsu VPP5000 computer.

References and Notes

1) Bartnik R., Orlowska B., *Polish J. Chem.*, **62**, 151—157 (1988).
2) Baas P., Cerfontain H., *Tetrahedron Lett.*, **17**, 1501—1504 (1978).
3) Brady O. L., Dunn F. P., *J. Chem. Soc.*, **103**, 1619—1626 (1913).
4) Niiya T., Ikeda H., Yukawa M., Goto Y., *Chem. Pharm. Bull.*, **45**, 1387—1392 (1997).
5) Pawar D., Mark H. L., Hosseini H., Harris Y., Noe E. A., *J. Phys. Chem.*, **97**, 7480—7483 (1993).
6) Maruzasa N., a master's thesis (2001) Graduate School of Pharmaceutical Sciences of Fukuoka University.
7) Niiya T., Ikeda H., Yukawa M., Goto Y., *Chem. Pharm. Bull.*, **49**, 473—475 (2001).
8) Ikeda H., Yukawa M., Niiya T., Goto Y., *Chem. Pharm. Bull.*, **49**, 1651—1652 (2001).
9) Frisch M. J., Trucks G. W., Schlegel H. B., Scuseria G. E., Robb M. A., Cheeseman J. R., Zakrzewski V. G., Montgomery J. A., Jr., Stratmann R. E., Burant J. C., Dapprich S., Millam J. M., Daniels A., D., Kudin K. N., Strain M. C., Farkas O., Tomasi J., Barone V., Cossi M., Cammi R., Mennucci B., Pomelli C., Adamo C., Clifford S., Ochterski J., Petersson G. A., Ayala P. Y., Cui Q., Morokuma K., Malick D. K., Rabuck A. D., Raghavachari K., Foresman J. B., Cioslowski J., Ortiz J. V., Baboul A. G., Stefanov B. B., Liu G., Liashenko A., Piskorz P., Komaromi I., Gomperts R., Martin R. L., Fox D. J., Keith T., Al-Laham M. A., Peng C. Y., Nanayakkara A., Challacombe M., Gill P. M. W., Johnson B., Chen W., Wong M. W., Andres J. L., Gonzalez C., Head-Gordon M., Replogle E. S., Pople J. A., "Gaussian 98," Revision A.9; Gaussian, Inc., Pittsburgh PA, 1998.